Arc Repressor−Operator DNA Interactions and Contribution of Phe10 to Binding Specificity†

Lubomír Dostál, Rolf Misselwitz, and Heinz Welfle*

AG Biopolymerspektroskopie, Max-Delbrück-Centrum für Molekulare Medizin Berlin-Buch, Robert-Rössle-Strasse 10, D-13092 Berlin, Germany

Received November 12, 2004; Revised Manuscript Received April 14, 2005

ABSTRACT: Solution properties of Arc repressors (wild-type and F10H variant) from *Salmonella* bacteriophage P22 and their complexes with operator DNA (Arc-wt−DNA and Arc-F10H−DNA) were characterized by circular dichroism, fluorescence, and Raman difference spectroscopy and compared with the crystal structures of free and DNA-bound Arc repressors (wild-type and F10V variant). From the crystal structure of Arc-wt−operator DNA complex, it is known that amino acids Phe10/10′ flip out of the hydrophobic protein core, and in the Arc-F10V−DNA complex, the methyl groups of Val10/10′ rotate toward the DNA. Arc-wt and Arc-F10H significantly perturb the Raman signatures of the operator DNA upon complex formation. The two proteins induce similar changes in the DNA spectra. Raman markers in the difference spectra (spectrum of the complex minus spectra of DNA and Arc) indicate binding of Arc in the major groove, several direct contacts, e.g., hydrogen bonds of protein residues with bases, and slight perturbations of the deoxyribose ring systems that are consistent with bending of the operator DNA. Trp14, the only one tryptophan of Arc repressor monomers, serves as a very sensitive tool for changes of the hydrophobic core of the protein. The Raman spectra identify in the free Arc-F10H variant a largely different $\chi^{2,1}$ rotation angle of Trp14 compared to that in wild-type Arc. In the Arc-wt−DNA and Arc-F10H−DNA complexes, however, the Trp14 $\chi^{2,1}$ rotation angles are similar in both proteins. Furthermore, in both complexes, a strengthening of the van der Waals interactions of the aromatic ring of Trp14 is indicated compared to these interactions in the free proteins. According to the fluorescence and Raman data, His10 is buried in the hydrophobic core of free Arc-F10H, resembling the "core" conformation of Phe10 in Arc-wt, but His10 is looped out in the complex with DNA resembling the "bound" conformation of Phe10 in the Arc-wt−operator DNA complex.

Wild-type Arc repressor (Arc-wt)[1] of *Salmonella* bacteriophage P22 is involved in the switch between the lysogenic and lytic pathways of P22 by regulating the transcription of the *ant* gene during lytic growth (*1*). Arc-wt is a small homodimeric protein and belongs to the MetJ/Arc structural superfamily. Proteins of this family form a ribbon−helix−helix DNA-binding motif (*2*). In the cocrystal structure, two Arc dimers bind to adjacent subsites of a 21-bp operator DNA (Figure 1A). An antiparallel β sheet of Arc recognizes bases in the major groove, and N-terminal arms contribute to the interaction by direct contacts with DNA subsites (*3*). Arc-wt and Arc-F10V (Arc repressor variant with Val instead of Phe in position 10) complexes with operator DNA form very similar structures (*3*−*4*). An extraordinary feature is observed in the crystal structures of the Arc-wt−DNA complex, namely, the protrusion of the aromatic rings of Phe10 and Phe10′ and their packing against phosphate oxygens and ribose atoms of the DNA backbone (Figure 1B) (*3*). A conformational change of the side chains of Val10/10′ is also visible in the crystal structure of the Arc-F10V−DNA complex (PDB file 1BAZ) (*4*). Previous studies have shown that mutations at Phe10 reduce operator binding and protein stability (*5*−*6*). Furthermore, three Phe10 mutants were probed that produced stably folded proteins with partial activity in the cell. These studies demonstrated that Phe10 is essential for high-affinity binding of Arc to its operator DNA and contributes to the discrimination between operator and nonoperator DNA (*4*). In free form, Arc-wt is the most stable Arc variant followed by Arc-F10V, Arc-F10Y, and Arc-F10H. Interestingly, Arc-F10H is the least stable free protein, but it forms the most stable complex with operator DNA out of all tested Arc Phe10 mutants (*4*).

Solution structures of Arc-wt and Arc-MYL (with amino acid exchanges R31M/E36Y/R40L) and the dynamics of Phe10 in these proteins were studied by NMR spectroscopy (*7*−*9*). In the free Arc repressor dimer, at and below room temperature, Phe10 exists predominantly in the "core" conformation, where it is buried in a hydrophobic core (12% solvent accessibility). Only the core conformation is observed in the crystal structure of hyper stable variant Arc-P8L, where

† This work was supported by the Deutsche Forschungsgemeinschaft (Graduiertenkolleg GK 80/3, partial project to H.W.), by the EU project QLK3-CT-2001-00277, and by a grant from the Spanish Ministerio de Educacion y Ciencia to H.W.

* To whom correspondence should be addressed: Max-Delbrück-Centrum für Molekulare Medizin Berlin-Buch, Postfach 740238, D-13092 Berlin, Germany. E-mail: welfle@mdc-berlin.de. Fax/Telephone: +49-30-9406-2840.

[1] Abbreviations: Arc-wt, wild-type Arc repressor; Arc-F10H, Arc repressor variant with His instead of Phe in position 10; Arc-wt−DNA, complex of Arc-wt with operator DNA; Arc-F10H−DNA, complex of Arc-F10H variant with operator DNA.

10.1021/bi0476073 CCC: $30.25
Published on Web 05/20/2005

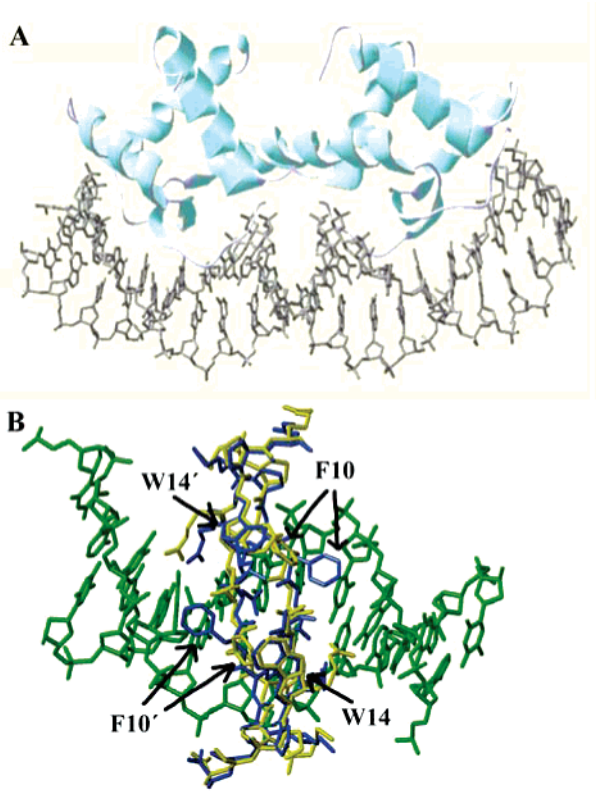

FIGURE 1: (A) Model of the Arc-wt−operator DNA complex. (B) Superposition of amino acids 7−16 of Arc-wt in "bound" (blue) and "core" (yellow) conformation. The figures were prepared using SPDBV (DeepView/Swiss-PdbViewer from http://www.expasy.org/spdb/) and the atomic coordinates from PDB files 1PAR and 1ARR.

Pro8 is substituted by Leu8 (*10*). In solutions of Arc-wt and Arc-MYL, a second, less stable "bound" conformation (similar to the conformation found in the Arc repressor−operator DNA complex) with protruded Phe residues coexists with the "core" conformation. In the crystal structure, however, Arc-MYL (PDB file 1MYL) exists only in a "bound" conformation (*7*−*9*).

The structures of free Arc-wt (1PAR) and Arc-F10V (1BAZ) are similar. Amino acid F10 has a decisive effect on complex formation with DNA, and mutating of F10 has consequences both on stability and function of Arc repressor. To understand the importance of amino acids in position 10 for a specific and high-affinity binding of Arc repressor to its operator DNA and to gain a better understanding of the nature of the conformational differences of Arc variants and their operator DNA complexes, we analyzed and assigned structural/dynamic changes that correlate with functional observations by comparing circular dichroic, fluorescence, and Raman spectroscopic results of Arc-wt and Arc-F10H. We obtained spectroscopic evidence that His10/10′, like amino acids Phe10/10′ and Val10/10′, change their conformation when bound to DNA. We discuss the solution structures of free and operator-bound Arc-F10H based on all available spectral perturbations and the contribution of Phe10 to the specificity of operator DNA binding.

MATERIALS AND METHODS

Chemicals. Isopropyl-β-D-thiogalactopyranoside (IPTG), ampicillin, and ultrapure acrylamide were obtained from Roth, Karlsruhe, Germany. All other chemicals were purchased from Merck, Darmstadt, Germany. Phosphocellulose was from Whatman, Maidstone, U.K. Superdex 200, SP-sepharose, and heparin-sepharose were from Amersham-Pharmacia, Freiburg, Germany.

Preparation of Arc-wt, Arc-F10H, Operator DNA, Arc-wt−Operator DNA, and Arc-F10H−Operator DNA. Arc proteins were overexpressed in *Escherichia coli* X90(DE3) cells carrying plasmid pSA300, after induction with IPTG, and purified with some modifications as described elsewhere (*1*). Prior to spectroscopic measurements, Arc-wt and Arc-F10H were extensively dialyzed against 50 mM Tris/HCl, 100 mM KCl, and 10 mM $MgCl_2$ at pH 7.5 (buffer I), concentrated (Millipore filter device, Millipore, Bedford, MA), and gel-filtered on a Superdex 200 column, equilibrated with buffer I. Protein concentrations were determined from the absorbance at 278 nm using for both proteins an absorption coefficient of $\epsilon_{278\ nm} = 7000\ M^{-1}\ cm^{-1}$ calculated from the amino acid sequence with the Expasy server.

Oligonucleotides were purchased from the Department of Functional Genomics and Proteomics of the Masaryk University Brno, Czech Republic. Equimolar amounts of each strand were mixed, heated to 95 °C for 10 min, annealed by slow cooling, purified by gel filtration using a Superdex 200 column equilibrated in buffer I, and concentrated. Concentrations of operator DNA were determined spectrophotometrically using an extinction coefficient $\epsilon_{260\ nm} = 12\ 690\ M\ bp^{-1}\ cm^{-1}$ calculated from the base composition according to ref *11*.

Complexes of Arc-wt and Arc-F10H with operator DNA (Arc-wt−DNA and Arc-F10H−DNA) were prepared by mixing proteins and DNA in a 2:1 molar ratio. The solutions were incubated before measurements for at least 12 h.

Circular Dichroism (CD) and Fluorescence Measurements. CD spectra in the far-ultraviolet region were obtained with a Jasco-J720 spectropolarimeter using 0.01 cm pathlength quartz cuvettes at 23 °C. Protein samples (~0.6 mg/mL) were in buffer I.

Tryptophan fluorescence spectra were obtained with a Jasco-FP6500 spectrofluorimeter at an excitation wavelength of 280 nm and with 1 and 5 nm bandwidths for the excitation and emission monochromators, respectively. Proteins (~0.09 mg/mL) and complexes (~0.13 mg/mL) were in buffer I.

Raman Spectroscopy. Homemade quartz cuvettes were filled with approximately 12 μL sample solution and then tightly closed with Teflon stoppers. The sample concentrations were 16 and 24 mg/mL for operator DNA, 27 and 20 mg/mL for Arc-wt, and 43 and 35 mg/mL for the Arc-wt−DNA complex. In the measurements with Arc-F10H, the concentrations are 24 mg/mL for operator DNA, 41 mg/mL for Arc-F10H, and 65 mg/mL for the Arc-F10H−DNA complex. Spectra were collected at 22 °C on the Raman spectrometer T64000 (Jobin Yvon, France) in single-mono configuration equipped with a liquid nitrogen-cooled charge-coupled-device (CCD) detector. The 488 nm line of a Coherent Innova 90 argon ion laser with 100 mW of radiant power at the sample position in the macrochamber was used for the excitation of the Raman spectra. A total of 10 spectra, each measured for 300 s, were accumulated and averaged to produce the spectra shown in Figures 3−5. To exclude all possible drifts of the wavenumber scale during the data measurement, a calibration spectrum was collected after each

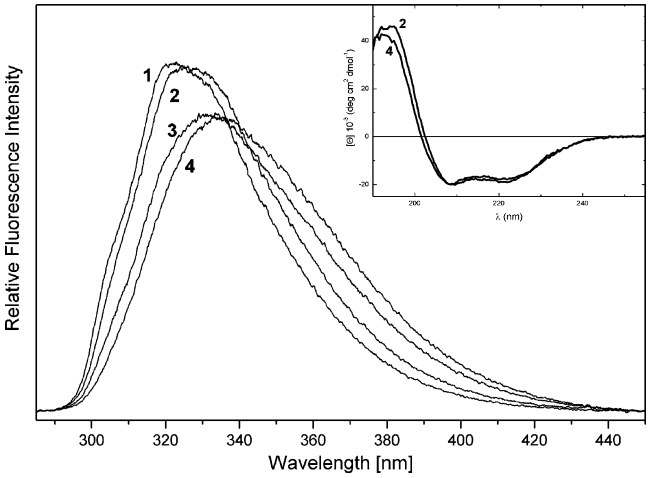

FIGURE 2: Fluorescence spectra (285−450 nm, 280 nm excitation) of the Arc-wt−operator DNA complex (trace 1), the Arc-wt (trace 2), the Arc-F10H−operator DNA complex (trace 3), and the Arc-F10H (trace 4). The concentrations of the samples were ∼0.09 mg/mL for proteins and ∼0.13 mg/mL for complexes. (Inset) CD spectra of the Arc-wt (trace 2, corresponding to fluorescence spectrum 2) and the Arc-F10H (trace 4, corresponding to fluorescence spectrum 4), with the sample concentration at ∼0.6 mg/mL. Fluorescence and CD data were collected in 50 mM Tris/HCl, 100 mM KCl, and 10 mM $MgCl_2$ at pH = 7.4 and 23 °C.

300 s sample spectra accumulation step. The calibration procedure is described in detail elsewhere (*12*).

Raman data analyses were performed with the software packages LabSpec (Jobin Yvon) and GRAMS (Thermo Galactic). Minimization of intensity differences between the spectra of isolated components and Arc-operator DNA complexes is crucial for the calculation of difference spectra. To achieve this, the operator DNA spectrum was normalized with respect to the P−O stretching vibration of the phosphodioxy group (PO_2^-) near 1092 cm^{-1}; and the Arc spectrum was normalized with respect to the CH_2 scissoring vibration at 1445 cm^{-1}. Normalized but otherwise not corrected experimental spectra of operator DNA and Arc were subtracted from the spectrum of the Arc−operator DNA complex. In the next evaluation steps, contributions of buffer spectrum and fluorescence background were removed.

Difference bands were considered as significant when the following criteria are fulfilled: (i) the intensity of the difference band is at least 2 times higher than the signal-to-noise ratio, and (ii) the difference band reflects an intensity change of at least 5% of its parent band.

RESULTS

Fluorescence and CD Measurements of Arc and Arc−Operator DNA Complexes. Figure 2 shows tryptophan fluorescence spectra of Arc-wt (trace 2), Arc-F10H (trace 4), and Arc-wt− and Arc-F10H−operator DNA complexes (traces 1 and 3). The peak positions of the Arc-wt (327 nm) and Arc-F10H (333 nm) fluorescence spectra differ by ∼6 nm, indicating that the mutation of phenylalanine to histidine significantly decreases the hydrophobicity of the Trp14 environment. This mainly reflects the more hydrophilic nature of histidine compared to phenylalanine but not an increased exposition to the solvent. In the complexes with operator DNA, the fluorescence spectra of both complexes downshift for ∼2 nm. Thus, the Trp14 environment becomes slightly more hydrophobic. The inset of Figure 2 shows very similar CD spectra of Arc-wt (trace 2) and Arc-F10H (trace 4) that exhibit only a minor wavelength shift of the zero point transition, indicating very similar secondary structures of the two proteins.

Raman Signature of Arc-wt and Arc-F10H Repressor Proteins. Figure 3 shows the Raman spectra of Arc-wt (solid trace) and Arc-F10H (dashed trace). The spectra are characterized by strong amide I bands (1640−1680 cm^{-1}) centered near 1650 cm^{-1} and by complex amide III bands (1230−1310 cm^{-1}). For a more detailed comparison of the two Raman spectra, a difference spectrum was computed (Figure 3, bottom trace) by subtraction of the Arc-F10H spectrum from that of Arc-wt. A positive difference peak indicates higher Raman intensity in the spectrum of Arc-wt compared to the intensity at the corresponding position in the spectrum of Arc-F10H, and a negative difference trough is caused by lower intensity in the spectrum of Arc-wt and higher intensity in the spectrum of Arc-F10H.

Phenylalanine. The difference peaks near 621, 1003, 1032, 1211, 1587, and 1606 cm^{-1} indicate Phe vibrations and reflect the fact that Phe residues (Phe10/10′) are present in Arc-wt but not in Arc-F10H.

Environment of Tyrosine Side Chains. Tyrosine forms a doublet in the Raman spectrum of Arc-wt with a very sharp, relatively intensive peak at 851 cm^{-1} and a smaller and broader band at 823 cm^{-1} (Figure 3, solid trace). The intensity ratio I_{851}/I_{823} has an extraordinarily high number of 2.9. This points to the formation of a very strong hydrogen bond with the phenoxyl oxygen of tyrosine as an acceptor (*13*). In Arc-F10H, the higher wavenumber component of the tyrosine doublet changes its frequency as indicated by the peak/trough feature at 853/848 in the difference spectrum (Figure 3, bottom trace). The intensity of the band remains the same; thus, the difference feature does not reflect a change in the hydrogen-bonding state of the Tyr residues in the mutant protein.

Tryptophan. Both Arc-wt and Arc-F10H contain a unique Trp14/14′ that is localized in the DNA-binding β sheet of the protein. The Trp band near 1549 cm^{-1} (called W3 mode) assumes wavenumber values between 1542 and 1557 cm^{-1} depending on the absolute value of the $C_\alpha C_\beta - C_3 C_2$ torsion angle $|\chi^{2,1}|$, which usually varies between 60° and 120°. According to ref *17*, the torsion angle $|\chi^{2,1}|$ can be calculated from experimentally determined wavenumber X of the W3 mode using the empirical equation: $X = 1542 + 6.7(\cos 3|\chi^{2,1}| + 1)^{1,2}$. In the Arc-F10H spectrum, the band is positioned at 1555 ± 0.5 cm^{-1}. This wavenumber position corresponds to an average $|\chi^{2,1}|$ value of ∼106°. In the Arc-wt spectrum, the band has the extreme position of 1559 ± 0.5 cm^{-1}, and the protein difference spectrum shows a very prominent difference peak/trough feature at 1561/1552 cm^{-1} with 35% relative intensity change compared to the parent band of Arc-wt. This observation suggests a large conformational difference for Trp14/14′ in Arc-wt and Arc-F10H. Unfortunately, for extreme wavenumbers below 1542 and above 1557 cm^{-1}, the empirical equation given above is not applicable because the calculation would result in senseless absolute values >1 for the cosinus function. Therefore, $|\chi^{2,1}|$ cannot be calculated in the usual manner. However, the NMR structure of Arc-wt (PDB file 1ARR) shows a value of $\chi^{2,1}$ of approximately −9°. From the NMR data of Arc-wt and

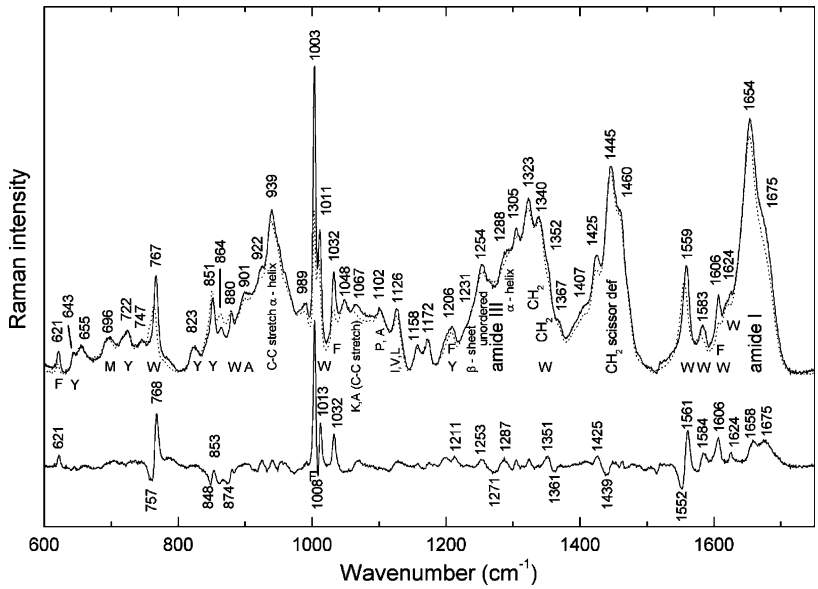

FIGURE 3: Raman spectra in the region 600−1750 cm^{-1}. The spectra at the top are that of Arc-wt (solid trace) and Arc-F10H (dashed trace). The bottom trace shows the Raman difference spectrum (solid trace minus dashed trace). Samples contained 20 and 41 mg/mL of the Arc-wt and the Arc-F10H, respectively, in 50 mM Tris/HCl, 100 mM KCl, and 10 mM $MgCl_2$ at pH 7.4. The samples were excited at 488 nm, and the data were collected at 22 °C. Spectra were normalized with respect to the CH_2 scissoring vibration at 1445 cm^{-1}. Raman band assignments to amino acids (one letter code) or amide vibrations are from refs *14*−*16*.

the Raman data of Arc-F10H follows that a point mutation in the neighborhood of Trp14/14′ results in a very remarkable rotation of the Trp residue from −9° in Arc-wt to ∼|106°| in Arc-F10H.

The Trp vibrations are very sensitive to the indole ring environment. In Arc-wt, the position of the indole ring vibration at 880 cm^{-1} (called W17 mode) is indicative for a buried Trp residue with an exocyclic 1NH group that is not (or only weakly) participating in hydrogen-bond formation (*18*). The positions and intensities of the W17 bands differ in the spectra of Arc-wt and Arc-F10H, resulting in the difference trough at 874 cm^{-1} (Figure 3, dashed trace). This feature indicates that Trp14/14′ form in Arc-F10H obviously stronger hydrogen bonds than in Arc-wt. The observation correlates with the perturbation of the $|\chi^{2,1}|$ angle described before.

Hydrophobic interactions may influence the hydrogen-bonding state of Trp14/14′. For model compounds in solution, the components of the Fermi doublet of tryptophan are found at about 1360 and 1340 cm^{-1}. The intensity ratio $R = I_{1360}/I_{1340}$ serves as a hydrophobicity marker. The 1360 cm^{-1} component of the doublet is strong in hydrophobic solvents, whereas in the hydrophilic environment, the 1340 cm^{-1} component is stronger. R is below 0.9 for hydrophilic solvents and higher than 1.1 for hydrophobic solvents (*18*). The intensity ratio cannot be determined in most protein spectra because of overlapping of the Trp doublet with bands caused by CH-bending vibrations of aliphatic side chains. In the difference spectrum obtained by subtraction of the Arc-F10H spectrum from that of the Arc-wt spectrum, the intensity difference of the Fermi doublets could be detected as a trough/peak feature at 1361/1351 cm^{-1} because of the elimination of all other signals. The trough/peak feature is probably caused by an upshift of the 1360 cm^{-1} component. An alternative explanation is in contradiction with the fluorescence measurements (see Figure 2), namely, a higher intensity of the 1360 cm^{-1} component and a lower intensity of the 1340 cm^{-1} component because of a more hydrophobic environment of the indole ring environment in Arc-F10H.

The very strong Trp band near 761 cm^{-1} (W18 mode) is a sensitive marker to the amphipathicity of the environment of the indole ring (*19*). A tryptophan side chain in the hydrophilic environment gives rise to a very strong band, while in the hydrophobic environment, the band becomes weaker (*19*). In the Arc-wt spectrum, a very strong and sharp band is located at 767 cm^{-1}. In the Arc-F10H spectrum, the band loses 35% of its relative intensity, whereas a weak shoulder at 757 cm^{-1} increases its intensity. These changes result in a peak/trough feature (768/757 cm^{-1}) of the protein difference spectrum.

The F10H mutation produces a downshift of the W16 mode from 1011.5 (Arc-wt) to 1010 cm^{-1} (Arc-F10H) and results in a peak/trough feature at 1013/1008 cm^{-1}. Environment effects on the position of the W16 mode were studied for several crystalline tryptophan derivatives (*17*). However, to our knowledge, environmental effects on the intensity or position of this band have not been elucidated for solution conditions.

Raman Signature of the Arc Repressor Operator DNA. Figure 4 shows the Raman spectrum and the sequence of the 22-mer operator site DNA (21-bp and one base 5′ overhang) in the 600−1750 cm^{-1} wavenumber region. The sequence of the oligonucleotide is exactly that used in the crystallographic analysis of the Arc−operator DNA complex (*3*). Wavenumber positions and assignment of the major peaks are in accordance with those given previously in the literature (refs *20*−*23* and references therein). The backbone conformation markers at 833 and 1093 cm^{-1} are diagnostic of B DNA (*21*), and the nucleoside conformation markers at 669 cm^{-1} (dT), 683 cm^{-1} (dG), 729 cm^{-1} (dA), 751 cm^{-1} (dT), and 1256 cm^{-1} (dC) identify C2′-endo/anti conformers. The spectrum serves as basis for the interpretation of the difference spectra shown in Figure 5.

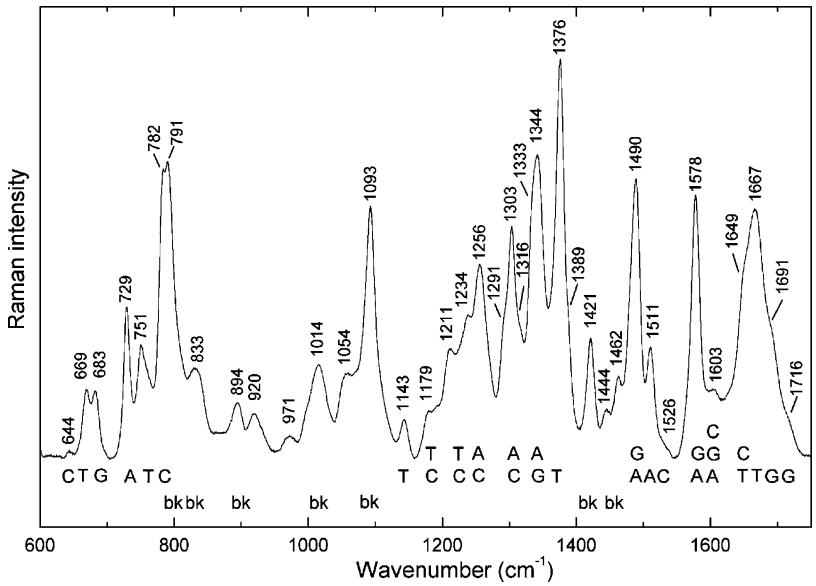

FIGURE 4: Raman spectrum of the 22-mer Arc repressor operator DNA at 24 mg/mL concentration. Experimental conditions are as given in the caption of Figure 3. Peak positions of prominent Raman bands are labeled. Abbreviations are as follows: G, guanine; T, thymine; C, cytosine; A, adenine; bk, deoxyribose backbone.

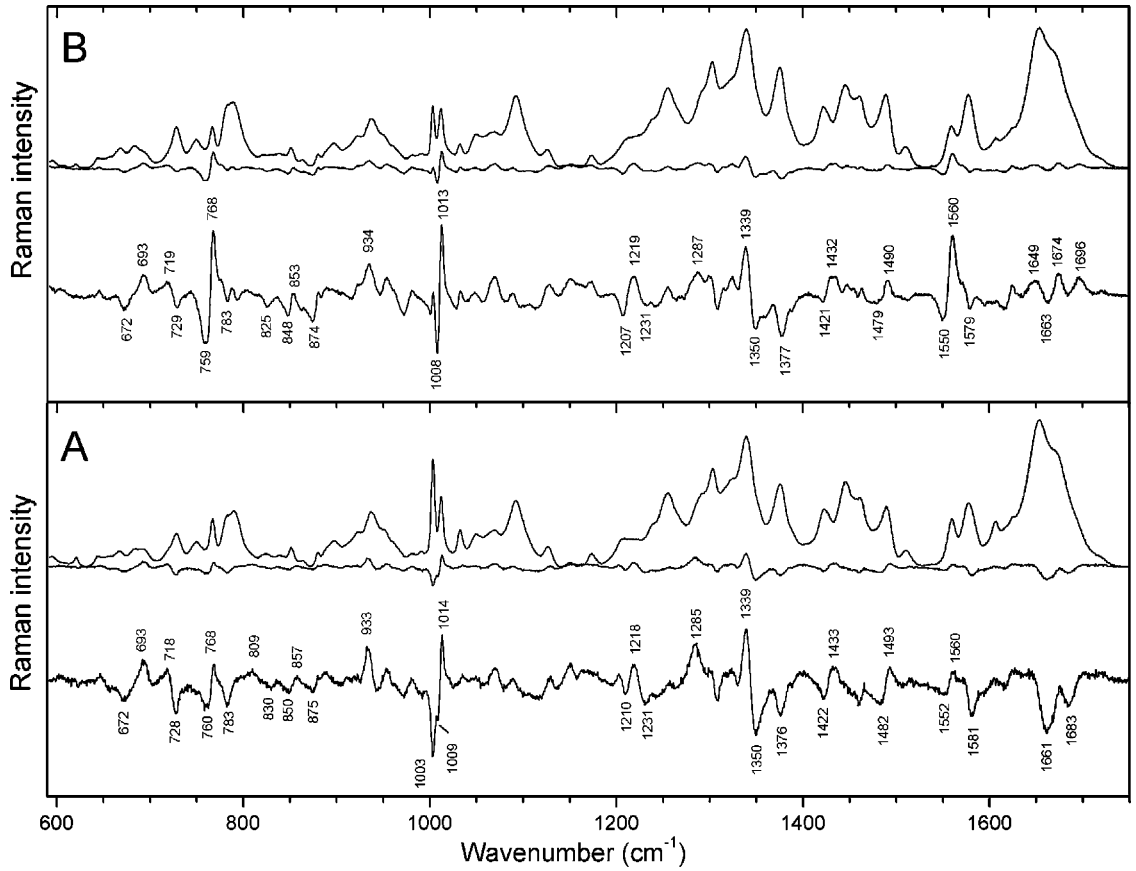

FIGURE 5: (A) Raman spectrum of the Arc-wt−operator DNA complex in a 2:1 molar ratio (top trace). Raman difference spectrum obtained by subtraction of the isolated component spectra from the experimental spectrum of the complex (middle trace) and 4 times enlarged difference spectrum (bottom trace). (B) Raman spectrum of the Arc-F10H−operator DNA complex in a 2:1 molar ratio (top trace). Raman difference spectrum obtained by subtraction of the isolated component spectra from the experimental spectrum of the complex (middle trace) and 4 times enlarged difference spectrum (bottom trace). Experimental conditions are as given in the caption of Figure 3.

Raman Analysis of the Arc Repressor−Operator DNA Complex. Figure 5 shows the Raman spectra of the complexes of Arc-wt (A, top trace) and Arc-F10H (B, top trace) with operator DNA. In A and B, the middle traces are the computed difference spectra that were obtained by subtraction of the component spectra (Figures 3 and 4) from the spectra of the complexes and the bottom traces show 4 times enlarged difference spectra. More than 30 Raman peaks and troughs in the difference spectra demonstrate structural perturbations as a result of the complex formation. The most important difference peaks and troughs are assigned and summarized in Table 1.

Table 1: Frequencies and Proposed Assignments for Raman Difference Bands of the Arc-F10H−DNA Complex[a]

wavenumber (cm^{-1}) or intensity shift	residue assignment[b]	inferred structure change
672 ↓	dT	altered deoxynucleoside conformation
693 ↑	dG	altered deoxynucleoside conformation
719 ← 729	dA	altered deoxynucleoside conformation
783 ↓	dC	altered deoxynucleoside conformation
825 ↓	O−P−O	modification of B-form DNA backbone
934 ↑	deoxyribose ring	DNA bending
1421 → 1432	deoxyribose ring	DNA bending
1479 → 1490	dG	guanine N7 interaction
1339 ← 1350	dA	adenine N6 and/or N7 interaction
759 → 768	Trp14	altered hydrophobic environment
874 ↓	Trp14	altered hydrophobic environment
1008 → 1013	Trp14	altered interaction with phenyl ring
1550 → 1560	Trp14	change in $\chi^{2,1}$ rotation angle
1003[c] ↓	Phe10	altered phenyl ring interaction
1649, 1674, 1696 ↑	amide I, dC, dG, dT	change in secondary structure of Arc and/or dC, dT, dG conformation
1663 ↓	amide I, dC, dG, dT	change in secondary structure of Arc and/or dC, dT, dG conformation

[a] Raman data are from the spectrum of Arc-F10H−DNA complex shown in Figure 5B. [b] Assignments to specific amino acid side chains are based upon literature data (*24*) and references therein. [c] Data are from the spectrum of Arc-wt−DNA complex shown in Figure 5A. The arrows →, ←, ↑, and ↓ show upshift, downshift, increase, and decrease of the band intensity, respectively.

(1) Backbone and Deoxynucleoside Conformation of the Operator DNA. In the 600−900 cm^{-1} region, Raman markers of deoxynucleoside conformation and DNA backbone geometry are located (*21*). The 782 cm^{-1} band in the Raman spectra of DNA is assigned to cytosine. The 791 cm^{-1} band is assigned to a stretching vibration of backbone phosphodiester groups and diagnostic of B-form DNA backbone geometry, specifically of torsion angles α and ζ in *gauche*$^-$ range (*25*−*27*). In DNA spectra, usually the cytosine and backbone bands overlap to one band near 784 cm^{-1}, whereas these bands are partially resolved in the spectrum of the Arc operator DNA. The difference trough near 783 cm^{-1} exhibits a decrease in the cytosine band intensity. A peak at 809 cm^{-1} and trough at 830 cm^{-1} in the difference spectrum of Arc-wt (Figure 5A) and a trough near 825 cm^{-1} in the difference spectrum of Arc-F10H (Figure 5B) result from changes in the broad B-DNA backbone band near 830 cm^{-1}.

The peaks at 669 (thymine) and 683 cm^{-1} (guanosine) in the spectrum of the operator DNA (Figure 4) are nucleoside conformation markers for B-form DNA and sensitive to altered deoxynucleoside conformation. In the difference spectrum, there is a trough at 672 cm^{-1} and a peak at 693 cm^{-1} (Figure 5A). A downward shift of the 729 cm^{-1} adenosine marker band is indicated by a difference feature with a peak near 718 and a trough near 728 cm^{-1}. Altogether, the difference features near 672, 693, 728, and 783 cm^{-1} are consistent with altered deoxynucleoside conformations of guanosine, thymidine, adenosine, and cytidine in the complex.

(2) Deoxyribose Ring and Protein CH_2/CH_3 Vibrations. Furanose vibrations were identified in Raman spectra of DNA near 930, 1420, and 1460 cm^{-1} and assigned to backbone vibrations (*25*, *28*−*29*). In the spectrum of the Arc operator DNA, the peak positions of those bands are at 920, 1421, and 1462 cm^{-1} (Figure 4). Protein bands overlap with DNA in these spectral regions. An intense band at 939 cm^{-1} is due to a C−C stretch of α helices; COO^- symmetric stretch vibrations cause the 1402 cm^{-1} peak; a band at 1424 cm^{-1} reflects CH_2 and CH_3 deformations; and at 1444 cm^{-1}, CH_2 scissoring modes are found (Figure 3). In Figure 5, the peak/trough feature at 1433/1422 cm^{-1} and a peak at 933 cm^{-1} may be assigned to backbone vibrations of the DNA and/or changes in the protein. The crystal structures of Arc-wt−DNA and Arc-F10V−DNA indicate that Arc repressor binding slightly bends the operator DNA (*3*−*4*). Alterations of DNA helix geometry may contribute to the spectral differences observed upon Arc binding (Figure 5). Changes in these spectral regions were observed upon formation of the SRY HMG box−DNA complex and were attributed to bending and/or unwinding of the DNA (*25*).

(3) Purine Environment. The crystal structure of an Arc-wt−DNA complex (Figure 1) shows several direct contacts between protein and purine moieties in the major groove (*3*). On the first half site of operator DNA, residues Arg13/13′ form hydrogen bonds with N7 and O6 of the two guanine bases. On the second half site, Arg13′ binds to adenine N7 instead of guanine N7. Gln9/9′ form specific hydrogen bonds to N6 and N7 of adenine (*3*).

In accordance with the crystal structure, we expect prominent Raman features assignable to major groove interaction with guanine and adenine (Figure 5). A trough at 1482 cm^{-1} and a peak at 1493 cm^{-1} reflect hydrogen bonding to guanine N7 and upshifting of the guanine N7 band near 1490 cm^{-1}. A similar feature near 1490 cm^{-1} was recently observed in a KorB-N−DNA complex (*12*). The crystal structure of the KorB-N−DNA complex revealed direct contacts of the protein with guanine and cytosine bases in the major groove of the DNA (*30*). Cytosine does not contribute to the 1490 cm^{-1} band; therefore, the observed spectral feature can be correlated with guanine. The adenine band near 1344 cm^{-1} produces a prominent peak/trough feature at 1339/1350 cm^{-1} that indicates a direct contact of Arc with the $N6H_2$ and/or N7 positions of adenine; at present, we cannot discriminate between these two possibilities.

The guanine and adenine band at 1578 cm^{-1} results from the superposition of several components, one because of $N6H_2$ scissor vibration and others because of an adenine or guanine ring mode (*27*, *31*). The band exhibits a slight decrease in intensity at 1581 cm^{-1} after Arc repressor binding. In addition to guanine contributions, this intensity increase may result from adenine contributions.

(4) Pyrimidine Environment and Secondary Structure. Arc repressor contacts cytosines and thymines (*3*). Asn11 forms a hydrogen bond with cytosine $N4H_2$, and Asn11′ binds to

thymine O4. Thus, two contacts are formed to pyrimidines on each half-site of the operator, whereas four contacts are formed to purine bases.

At 1376 cm^{-1}, thymine exhibits a prominent Raman band of its exocyclic $C5H_3$ group. The intensity of the band increases with increasing hydrophilicity in the surrounding of $C5H_3$ and vice versa (*32*). The observed intensity decrease of the 1376 cm^{-1} band in the spectra of Arc-wt−DNA and Arc-F10H−DNA indicates increased hydrophobicity upon protein binding because of a more complete shielding from the solvent. The close neighborhood of the Arc Asn11′ NH_2 group to thymine O4 explains the observed hydrophobicity increase. Thymine C4═O Raman bands are located at 1649 and 1667 cm^{-1} (*27*, *31*). In the spectrum of Arc-wt−DNA, the thymine bands overlap with amide I bands of Arc. Figure 5A shows a trough at 1661 cm^{-1}, and Figure 5B shows a complicated feature with two peaks at 1674 and 1649 cm^{-1} and a trough at 1663 cm^{-1}. Amide I bands reflect secondary-structure elements of the proteins. Minor differences in the conformations of free Arc-wt and Arc-F10H are indicated in their fluorescence and Raman spectra (Figures 2 and 3) and may persist or even be pronounced in the complexes as suggested by the amide I features of the difference spectra (Figure 5). However, the interpretation is not unequivocal because of overlapping contributions from thymine C4═O bands and amide I protein bands in this spectral region.

Raman bands in the interval 1300−1750 cm^{-1} are sensitive to specific interactions of protein residues and DNA bases (*22*−*23*, *33*−*34*). Cytosine has very weak bands in this region compared to adenine, guanine, and thymine. Between 1200 and 1300 cm^{-1}, cytosine bands overlap with bands of thymine. A peak/trough at 1285/1264 cm^{-1} and a trough/peak/trough feature at 1210/1218/1231 cm^{-1} are possible consequences of Arc interaction to cytosine. In this spectral region, amide III bands of the proteins overlap with DNA bands. In the spectrum of Arc-wt−DNA, the intensity at 1285 cm^{-1} is higher and the intensity at 1231 cm^{-1} is lower compared to that of Arc-F10H−DNA. These features indicate minor differences in the conformations of Arc-wt and Arc-F10H.

(5) Phenylalanine. Arc-wt contains four phenylalanines per dimer (Phe10/10′ and Phe45/45′). All four Phe residues are buried in the hydrophobic core. It is a remarkable structural feature of the complex that the side chains of Phe10 and Phe10′ flip out from the hydrophobic core and pack between phosphate oxygens of the operator DNA (*3*). The intensity of the ring breathing vibration is reduced in the complex in comparison to that of free Arc-wt as reflected in the difference spectrum (Figure 5A, bottom trace) by a trough at 1003 cm^{-1}.

(6) Tryptophan. Arc contains only the Trp residues Trp14/14′; this facilitates the detection of key tryptophan markers in the Arc−operator DNA complex. Trp14/14′ does not directly participate in the binding of the protein to the operator DNA (*3*). Nevertheless, Arc-wt and Arc-F10H binding to operator DNA result in spectral perturbations of tryptophan marker bands.

The perturbation of the W3 mode near 1559 cm^{-1} is connected with a perturbation of the $C_\alpha C_\beta - C_3 C_2$ torsion angle $|\chi^{2,1}|$. The change of the angle is probably small, because the position of the band remains near 1559 cm^{-1}. Angle $\chi^{2,1}$ has in solution an average value of −9° (NMR structure of Arc-wt, PDB code 1AAR); angles of −8° (1PAR) and −10° (1BDV) were identified in two crystal structures.

NMR data of Arc-wt indicate that Trp14/14′ are buried in a very strong hydrophobic environment. Each Trp ring is surrounded by the side chains of one phenylalanine, one tyrosine, one isoleucine, and three valines. Upon complex formation, Phe10 and Phe10′ move in such a way that the hydrophobicity of the environment of the Trp residues alters. The W17 mode decreases its intensity at 875 cm^{-1}; this reflects changes in the hydrogen-bonding state of Trp 1NH. The W18 mode shifts to a lower wavenumber and produces a peak/trough feature at 768/760 cm^{-1}. Both bands reflect a change in the hydrophobicity of the Trp environment. This is consistent with the fluorescence measurements that indicate an increased hydrophobicity in the Trp surrounding. The very sharp W16 mode downshifts upon complex formation as indicated by a peak/trough feature at 1013.5/1008.5 cm^{-1}. This effect is probably directly related to the movement of the Phe10/10′ side chains.

In free Arc-F10H, the His10/10′ residues disturb the surrounding of Trp14/14′ in the hydrophobic core. Subsequently, the Trp14/14′ rings change their positions relative to the neighbor residues. This is reflected in the Raman spectrum by a shift of the W3 mode to 1555 cm^{-1} compared to its position in the spectrum of Arc-wt (Figure 3). However, upon complex formation (Figure 5B), the W3 mode is located at 1559 cm^{-1}, i.e., at the same position as in Arc-wt, pointing to similar $\chi^{2,1}$ values of Trp14/14′ in free Arc-wt and in the DNA complexes of Arc-wt and Arc-F10H.

Another effect of complex formation is a change in the W18, W17, and W16 modes of Trp. The W18 mode gains intensity at 768 cm^{-1} and loses the 757 cm^{-1} shoulder; the peak/trough feature is located near 768/759 cm^{-1}. The intensity of the W17 mode decreases by as much as 30%, resulting in a trough at 874 cm^{-1}. The W16 mode upshifts from 1010 to near 1012 cm^{-1} close to its position in the Arc-wt−DNA complex. The observed spectral changes of the Trp modes upon complex formation might be the result of conformational changes of His10/10′ that, like the side chains of Phe10/10′ and Val10/10′, loop out of the hydrophobic core of the protein and thus change the surrounding of Trp14/14′.

(7) Tyrosine. Arc contains one unique tyrosine (Tyr38) per monomer. The OH group of Tyr38/38′ is located at the protein surface and probably forms very strong hydrogen bonds with solvent water molecules. Ring atoms of Tyr38/38′ are directed toward Trp14/14′. Similar peak/trough features at 853/848 cm^{-1} are observed in the DNA complexes of Arc-wt and Arc-F10H (Figure 5) and in the difference spectrum of the free proteins (Figure 3).

DISCUSSION

Arc-wt has the highest affinity to operator DNA followed by F10H, F10Y, and F10V. Phe10/10′ is an essential determinant to operator DNA-binding affinity and specificity (*4*). Free-energy measurements (*4*) revealed that the point mutations F10H, F10Y, and F10V reduce the free energies of their complexes with DNA by 2.3, 4.9, and 5.6 kcal/mol, respectively, in comparison to that of Arc-wt (*4*). A quantitative explanation of the stability differences remains elusive.

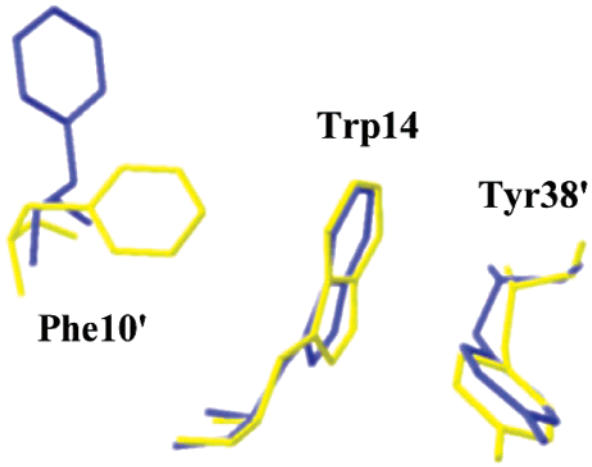

FIGURE 6: Superposition of Arc-wt amino acids Phe10′, Trp14, and Tyr38′ in "bound" (blue) and "core" (yellow) conformation. The figure was prepared using the atomic coordinates from PDB files 1PAR and 1ARR.

From the crystal structures of Arc-F10V and Arc-wt, it is known that the side chains of Val10/10′ and Phe10/10′ point similarly toward Trp14/14′. In the complex, Cγ^1 of Val10/10′ rotates out from the hydrophobic core (*4*). Similar considerations are reasonable for the positioning of His10/10′ and Tyr10/10′ in the Arc-F10H−DNA and Arc-F10Y−DNA complexes. The rings of His10/10′ and Tyr10/10′ might make contacts with phosphate oxygens in the complexes. However, the repulsion of the Tyr10 OH group and phosphates because of steric clash and/or unfavorable electrostatics is probably responsible for the lower binding energy of Arc-F10Y−DNA.

An essential aspect of the complex formation of Arc-wt with operator DNA is the movement of the Phe10/10′ side chains out of the hydrophobic core of the protein and their packing between phosphate oxygens of the operator DNA backbone (*3*). Substitution of Phe10 by a complete set of amino acids revealed several stable and partially active variants of Arc-wt (*4*), four of which were extensively studied (*4*−*5*). The Raman spectrum of the Arc-wt−DNA complex (Figure 5) shows a significant intensity reduction of intensity of the phenyl ring breathing vibration, which is a consequence of Phe10/10′ ring interaction and can be directly correlated with Phe10/10′ interactions in the "bound" conformation.

The completely water-excluded aromatic ring of Trp14 is located in the center of the hydrophobic core between Phe10′ and Tyr38′ (Figure 6) and is surrounded by one isoleucine and three valines. Trp14/14′ do not participate in direct interactions with DNA (*3*). Nevertheless, several Raman signals in difference spectra indicate a perturbed Trp14/14′ environment. The W16 mode of Trp14/14′ in the Arc-wt−DNA complex (Figure 5) demonstrates a pronounced effect of complex formation on the spectral properties of Trp14/14′. The Cζ-H atoms of Phe10/10′ are in 4-Å distance to the Trp14/14′ phenyl rings (PDB file 1BAZ); therefore, hydrogen bonds to the π electrons of the Trp14/14′ rings would be possible (*35*). However, the mutation of Phe10/10′ to Val10/10′ did not significantly decrease the free energy of the variant protein, which might occur if these hydrogen bonds exist in Arc-wt but not in the mutant. Similar peak/trough features assignable to the W16 mode of Trp14/14′ were observed in the Arc-F10H−DNA complex (Figure 5B) and in the Arc-wt−Arc-F10H difference spectrum (Figure 3). These spectroscopic observations may be explained in the following manner: in free Arc-F10H, the $|\chi^{2,1}|$ angle of Trp14/14′ is approximately 106° and is significantly different to that of −9° in Arc-wt; i.e., Trp14/14′ leave in Arc-F10H the proximity of Tyr38/38′ and lose van der Waals contacts. This structural change leads to a wavenumber downshift of the W16 mode in the Arc-wt minus Arc-F10H difference spectrum (Figure 3). In the complex, Trp14/14′ of Arc-F10H approach again a close neighborhood to Tyr38/38′ and restore van der Waals contacts. The wavenumber upshift found in the spectrum of the Arc-wt−DNA complex suggests a tight interaction of Trp14/14′ to Tyr38/38′. In the complex, the Cβ atom of Tyr38/38′ is 3.6 Å apart from Cϵ^2 of Trp14/14′, whereas in the free protein, the distance is 3.9 Å. We conclude that changes in the position of the W16 band reflect the strength of van der Waals interactions with the Trp14/14′ rings.

When Phe10/10′ move out of the hydrophobic core upon binding of Arc-wt to DNA, Trp14/14′ prefer to stay in proximity to Tyr38/38′ in a hydrophobic neighborhood rather than to move to any space that might have become accessible by the movement of Phe10/10′. The space originally occupied by Phe10/10′ residues is partially filled by adjacent hydrophobic residues in the Arc-wt−DNA complex (PDB file 1PAR), which is consistent with a small increase of hydrophobicity of Trp14 (Figure 2).

His mutation of residues Phe10/10′ increases the hydrophilicity of the Trp14/14′ environment (Figures 2 and 3). In the free Arc-F10H, Trp14/14′ are probably located between Tyr38/38′ and His10/10′. If the His10/10′ residues would mimic the "bound conformation" of Phe10/10′ residues and stay out of the protein core, the hydrophobic environment of Trp14/14′ would probably not change and spectra similar to that of Arc-wt and the Arc-wt−DNA complex would be expected. Upon complex formation, Trp14/14′ of the Arc-F10H variant move (Figure 5) to a more favorable position that seems to be similar to that occupied by Trp14/14′ of the Arc-wt−DNA complex.

In the free dimeric form, residues Phe10/10′ of Arc-wt protein are buried in the hydrophobic core and point at Trp14/14′ (*10*). Val, Tyr, or His mutations of Phe10/10′ reduce the stability of the free variant Arc proteins by only 0.2, 0.6, and 1.0 kcal/mol, respectively (*4*). Raman and fluorescence spectra (Figures 2 and 3), however, show a significant effect of the F10H mutation on the hydrophobic core. The Raman spectra indicate significant differences in the $\chi^{2,1}$ rotation angles of the Trp14/14′ residues in free Arc-wt and free Arc-F10H. Possibly, His10/10′ try to occupy the same space in the protein core as Phe10/10′. Concomitantly, Trp14/14′ take up modified positions in a now more hydrophilic environment. Consistent with those considerations is the observation that the free energy of Arc-F10H is more decreased as that of Arc-F10V compared to Arc-wt because Val10/10′ reduce the hydrophobicity of the Trp14/14′ environment (*4*) much less than the more hydrophilic His10/10′ (Figures 2 and 3).

We can only speculate why the modified position of Trp14/14′ in Arc-F10H is energetically favorable. As a fact, the presence of His10/10′ residues in the core of Arc-F10H reduces the hydrophobicity of the Trp14/14′ surrounding and thus induces changes in the positions of the hydrophobic

residues in the neighborhood of Trp14/14′ and Phe10/10′. This new conformational situation seems to result in more favorable interactions.

The Trp14/14′ residues assume very similar positions in free Arc-wt and in DNA-bound Arc-wt. Contrarily, Trp14/14′ assume a different position in free Arc-F10H, whereas the Raman features of the Arc-F10H−DNA complex suggest a position similar to that in Arc-wt. A reasonable explanation might be that, upon complex formation, the His10/10′ side chains behave similar to that of Phe10/10′, move out of the core, and restore, in the Arc-F10H−DNA complex, a wild-type-like neighborhood of Trp14/14′.

According to the fluorescence spectra, the hydrophobicity of the Trp14/14′ environment differs in the Arc-F10H− and Arc-wt−DNA complexes (Figure 2). However, as might be expected, the Trp14/14′ surrounding is more hydrophobic in both complexes compared to the free proteins.

Why do the amino acid side chains at position 10 loop out in complexes of Arc repressor with operator DNA? Apparently, looping out of the Phe10 side chain enhances the specific interaction with the DNA and results in energetically favorable complexes. Amino acids in position 10 are in the neighborhood of amino acids Gln9, Asn11, and Arg13 that make direct contacts with DNA by the formation of hydrogen bonds. A moderate rearrangement of the short DNA-binding β sheets of the proteins is indicated in the crystal structures of Arc-wt−DNA and Arc-F10V−DNA (*3*−*4*). These rearrangements are confirmed by the spectral differences in the amide I region of the Raman spectra of free and DNA-bound Arc-wt and Arc-F10H (Figure 5). Also, Trp14/14′ move closer to Tyr38/38′, and amino acids 10/10′ leave the hydrophobic core. With Phe or His in position 10, energetically favorable structures are formed. Val at position 10 cannot come into energetically favorable close distance to DNA phosphates; therefore, the binding affinity of Arc-F10V to operator DNA is much lower than that of Arc-wt and Arc-F10H.

ACKNOWLEDGMENT

The authors thank Dr. Robert T. Sauer (MIT, Boston, MA) for providing the clones for Arc repressor wild-type and variant Arc-F10H.

REFERENCES

1. Vershon, A. K., Youderian, P., Susskind, M. M., and Sauer, R. T. (1985) The bacteriophage P22 Arc and Mnt repressors, *J. Biol. Chem. 260*, 12124−12129.
2. Raumann, B. E., Brown, B. M., and Sauer, R. T. (1994) Major groove DNA recognition by β-sheets: The ribbon−helix−helix family of gene regulatory proteins, *Curr. Opin. Struct. Biol. 4*, 36−43.
3. Raumann, B. E., Rould, M. A., Pabo, C. O., and Sauer, R. T. (1994) DNA recognition by β-sheets in the Arc repressor-operator crystal structure, *Nature 367*, 754−757.
4. Schildbach, J. F., Karzai, A. W., Raumann, B. E., and Sauer, R. T. (1999) Origins of DNA-binding specificity: Role of protein contacts with DNA backbone, *Proc. Natl. Acad. Sci. U.S.A. 96*, 811−817.
5. Milla, M. E., Brown, B. M., and Sauer, R. T. (1994) Protein stability effects of a complete set of alanine substitutions in Arc repressor, *Nat. Struct. Biol. 1*, 518−523.
6. Brown, B. M., Milla, M. E., Smith, T. L., and Sauer, R. T. (1994) Scanning mutagenesis of the Arc repressor as functional probe of operator recognition, *Nat. Struct. Biol. 1*, 164−168.
7. Breg, J. N., van Ophesden, J. H. J., Burgering, M. J. M., Boelens, R., and Kaptein, R. (1990) Structure of Arc repressor in solution: Evidence for a family of β-sheet DNA-binding proteins, *Nature 346*, 586−589.
8. Bonvin, A. M. J. J., Vis, H., Breg, J. N., Burgering, M. J. M., Boelens, R., and Kaptein, R. (1994) Nuclear magnetic resonance solution structure of the Arc repressor using relaxation matrix calculations, *J. Mol. Biol. 236*, 328−341.
9. Nooren, I. M. A., Bietveld, A. W. M., Melacini, G., Sauer, R. T., Kaptein, R., and Boelens, R. (1999) The solution structure and dynamics of an Arc repressor mutant reveal premelting conformational changes related to DNA binding, *Biochemistry 38*, 6035−6042.
10. Schildbach, J. F., Milla, M. E., Jeffrey, P. D., Raumann, B. E., and Sauer, R. T. (1995) Crystal structure, folding, and operator binding of the hyperstable Arc repressor mutant PL8, *Biochemistry 34*, 1405−1412.
11. Bloomfield, V. A., Crothers, D. M., and Tinoco, I., Jr. (1999) Electronic and vibrational spectroscopy, in *Nucleic Acids, Structures, Properties, and Functions*, pp 165−221, University Science Books, Sausalito, CA.
12. Dostál, L., Khare, D., Bok, J., Heinemann, U., Lanka, E., and Welfle, H. (2003) RP4 repressor protein KorB binds to the major groove of the operator DNA: A Raman study, *Biochemistry 42*, 14476−14482.
13. Siamwiza, M. N., Lord, R. C., Chen, M. C., Takamatsu, T., Harada, I., Matsuura, H., and Shimanouchi, T. (1975) Interpretation of the doublet at 850 and 830 cm^{-1} in the Raman spectra of tyrosyl residues in proteins and certain model compounds, *Biochemistry 14*, 4870−4876.
14. Serban, D., Arcineigas, S. F., Vorgias, C. E., and Thomas, G. J., Jr. (2003) Structure and dynamics of the DNA-binding protein HU of *B. stearothermophilus* investigated by Raman and ultraviolet-resonance Raman spectroscopy, *Protein Sci. 12*, 861−870.
15. Overman, S. A., and Thomas, G. J., Jr. (1999) Raman markers of nonaromatic side chains in an α-helix assembly: Ala, Asp, Glu, Gly, Ile, Leu, Lys, Ser, and Val residues of phage fd subunits, *Biochemistry 38*, 4018−4027.
16. Overman, S. A., and Thomas, G. J., Jr. (1998) Amide modes of α-helix: Raman spectroscopy of filamentous virus fd containing peptide ^{13}C and ^{2}H labels in coat protein subunits, *Biochemistry 37*, 5654−5665.
17. Miura, T., Takeuchi, H., and Harada, I. (1989) Tryptophan Raman bands sensitive to hydrogen bonding and side-chain conformation, *J. Raman Spectrosc. 20*, 667−671.
18. Miura, T., Takeuchi, H., and Harada, I. (1988) Characterization of individual tryptophan side chains in proteins using Raman spectroscopy and hydrogen deuterium exchange kinetics, *Biochemistry 27*, 88−94.
19. Miura, T., Takeuchi, H., and Harada, I. (1991) Raman spectroscopic characterization of tryptophan side chains in lysozyme bound to inhibitors: Role of hydrophobic box in the enzymatic function, *Biochemistry 30*, 6074−6080.
20. Thomas, G. J., Jr., and Tsuboi M. (1993) Raman spectroscopy of nucleic acids and their complexes, *Adv. Biophys. Chem. 3*, 1−70.
21. Thomas, G. J., Jr., and Wang A. H.-J. (1988) Laser Raman spectroscopy of nucleic acids, *Nucleic Acids Mol. Biol. 2*, 1−30.
22. Benevides, J. M., Li, T., Lu, X.-J., Srinivasan, A. R., Olson, W. K., Weiss, M. A., and Thomas, G. J., Jr. (2000) Protein-directed DNA structure II. Raman spectroscopy of a leucine zipper bZIP complex, *Biochemistry 39*, 548−556.
23. Krafft, C., Hinrichs, W., Orth, P., Saenger, W., and Welfle, H. (1998) Interaction of Tet repressor with operator DNA and with tetracycline studied by infrared and Raman spectroscopy, *Biophys. J. 74*, 63−71.
24. Dostál, L., Chen, C. Y., Wang, A. H., and Welfle, H. (2004) Partial B-to-A DNA transition upon minor groove binding of protein Sac7d monitored by Raman spectroscopy, *Biochemistry 42*, 9600−9609.
25. Benevides, J. M., Chan, G., Lu, X.-J., Olson, W. K., Weiss, M. A., and Thomas, G. J., Jr. (2000) Protein-directed DNA structure. I. Raman spectroscopy of a high-mobility-group box with application to human sex reversal, *Biochemistry 39*, 537−547.
26. Benevides, J. M., Kukolj, G., Autexier, C., Aubrey, K. L., DuBow, M. S., and Thomas, G. J., Jr. (1994) Secondary structure and interaction of phage D108 Ner repressor with a 61-base-pair operator: Evidence for altered protein and DNA structures in the complex, *Biochemistry 33*, 10701−10710.
27. Movileanu, L., Benevides, J. M., and Thomas, G. J., Jr. (1999) Temperature dependence of the Raman spectrum of DNA. Part I.

Raman signatures of premelting and melting transitions of poly(dA-dT)·poly(dA-dT), *J. Raman Spectrosc. 30*, 637−649.
28. Prescott, B., Steinmetz, W., and Thomas, G. J., Jr (1984) Characterization of DNA structures by Raman spectroscopy, *Biopolymers 23*, 235−256.
29. Thomas, G. J., Jr, Benevides, J. M., Overman, S. A., Ueda, T., Ushizawa, K, Saitoh, M., and Tsuboi, M. (1995) Polarized Raman spectra of oriented fibres of A-DNA and B-DNA: Anisotropic and isotropic local Raman tensors of base and backbone vibrations, *Biophys. J. 68*, 1073−1088.
30. Khare, D., Ziegelin, G., Lanka, E., and Heinemann, U. (2004) Sequence-specific DNA binding determined by contacts outside the helix−turn−helix motif of the ParB homolog KorB, *Nat. Struct. Mol. Biol. 11*, 656−663.
31. Movileanu, L., Benevides, J. M., and Thomas, G. J., Jr. (2002) Temperature dependence of the Raman spectrum of DNA. II. Raman signatures of premelting and melting transitions of poly(dA)·poly(dT) and comparison with poly(dA-dT)·poly(dA-dT), *Biopolymers 63*, 181−194.
32. Benevides, J. M., Weiss, M. A., and Thomas, G. J., Jr. (1991) DNA recognition by the helix−turn−helix motif: Investigation by laser Raman spectroscopy of the phage λ repressor and its interaction with operator sites O_L1 and O_R3, *Biochemistry 30*, 5955−5963.
33. Benevides, J. M., Weiss M. A., and Thomas G. J., Jr. (1991) Design of the helix−turn−helix motif: Nonlocal effects of quaternary structure in DNA recognition investigated by laser Raman spectroscopy, *Biochemistry 30*, 4381−4388.
34. Benevides, J. M., Weiss, M. A., and Thomas, G. J., Jr. (1994) An altered specificity mutation in the λ repressor induces global reorganization of the protein−DNA interface, *J. Biol. Chem. 269*, 10869−10878.
35. Steiner, T., and Koellner, G. (2001) Hydrogen bonds with π-acceptors in proteins: Frequencies and role in stabilizing local 3D structures, *J. Mol. Biol. 305*, 535−557.

BI0476073